Available online at www.sciencedirect.com
SCIENCE DIRECT®
Polymer 44 (2003) 7251–7264
polymer
www.elsevier.com/locate/polymer

Molecular orientation and relaxation in poly(butylene terephthalate)/polycarbonate blends

A.K. Kalkar[a,*], H.W. Siesler[b], F. Pfeifer[b], S.A. Wadekar[a]

[a]*Applied Physics Division, Institute of Chemical Technology, University of Mumbai, Matunga, Mumbai 400019, India*
[b]*Department of Physical Chemistry, University of Essen, D45177 Essen, Germany*

Received 18 December 2002; received in revised form 3 July 2003; accepted 5 August 2003

Abstract

Rheo-optical Fourier-transform infrared (FTIR) spectroscopy is based on the simultaneous acquisition of stress–strain data and FTIR spectra on-line to the mechanical treatment of polymers and is frequently applied for the characterization of transient structural changes during deformation and stress-relaxation. In the present communication, this technique has been employed in order to investigate the distribution of molecular orientation and its relaxation in uniaxially drawn solution-cast films of semicrystalline partial miscible blends of poly(butylene terephthalate) (PBT) with polycarbonate (PC) containing 10, 30 and 50 wt% PC. The uniaxial deformation of these blend films having a PBT-crystallinity degree ranging from 31 to 12%, in unstretched blends, leads to a appreciable high segmental orientation for the crystalline PBT due to a structural transformation from lamellae to microfibrils. The formation of this fibrillar structure is attributed to non-reversibility of an extended phase with all-*trans* conformational sequence of the aliphatic segments of PBT, occurring during elongation. The rate of relaxation of this conformational transition, however, increases with increasing amorphous content in the blends. Also it is observed that even with increasing amorphous content in the PBT/PC blends the crystalline PBT shows significant orientation. In such cases, apart from the few lamellae which transform to microfibrils, it is suggested that a stress induced transformation of PBT chains in amorphous PBT-component to irreversible all-*trans* extended crystalline form also contributes to PBT crystalline orientation. In contrast with this high crystalline orientation, the amorphous PBT located in the interlamellar regions inside the PBT-spherulites show a lower orientation in blends as compared in pure PBT.

On the other hand, an overall segmental orientation of PC chains in blends is of lower order which is attributed mainly to low stretching temperature compared to T_g of pure PC. The results are discussed in terms of the resulting spherulitic morphology and the temporary network formed by the elongated PBT and PC chains inside the interlamellar regions, in blends.

Keywords: Rheo-optical Fourier-transform infrared spectroscopy; Orientation; Infrared dichroism

1. Introduction

It is well known that the mechanical properties of polymers are strongly influenced by an induced molecular orientation occurring under various polymer processing conditions. During such macroscopic deformation, the orientation of isotropic network of polymer chain segments becomes anisotropic with ability to adopt different conformations, from a coil to an extended chain. The state of anisotropy and the relaxation of these conformational changes determine to the greatest extend the mechanical properties particularly in the semicrystalline and liquid crystalline polymers. Thus, the characterization of molecular orientation and relaxation behaviour under strain is of a particular interest for both industrial applications and fundamental understanding of the molecular mechanisms involved in the polymer deformation [1,2]. Several experimental techniques such as X-ray diffraction, NMR spectroscopy, fluorescence polarization, polarized infrared and Raman dichroism, birefringence and polarization modulation methods (infrared dichroism or Raman) have been applied extensively to measure the orientation in polymers on a molecular scale in order to correlate the orientation behaviour and the morphological structure to mechanical properties [1–16]

The deformation mechanism involved in polymer blends are complex. The basic understanding of the mechanisms

* Corresponding author. Fax: +91-22-24145614.
E-mail address: drkalkar@vsnl.com (A.K. Kalkar).

0032-3861/$ - see front matter © 2003 Published by Elsevier Ltd.
doi:10.1016/j.polymer.2003.08.018

involved in orientation and its subsequent relaxation is based on the reptation theory of de Gennes [17] and on the chain relaxation model developed by Doi and Edwards [18,19]. In this model, the environment of a polymer chain is expressed in terms of a tube of neighbouring chain constraints in which the chain relaxes locally and finally reptates.

In the miscible blends the chain dynamics and the intermolecular interaction are two dominating factors [7, 20–27]. However, in the immiscible blends with two-phase microstructure, the deformation temperature has a significant effect on the orientation behaviour [28,29]. In such systems, the phase separated blend component domains are found to act as voids or rigid droplets in the another component matrix, depending on the deformation temperature above or below the glass transition temperature (T_g) of that component [28,29]. On the other hand, in partially miscible blends an additional contribution which accounts for the interpenetration induced interaction between the blend components must be taken into account, where the entanglement dependent network density of the two components in the blends influences the stretching induced orientation [22].

There have been very few studies on the orientation behaviour of immiscible polymer blends [30–36]. In most of these cases, it is observed that the major component orients to a higher degree than the minor dispersed component, which is again dependent on the stretching temperature [30,35,37]. The resultant morphology has a significant effect on the overall deformation behaviour, including the dynamics of the relaxations of these blends. The situation, however, becomes still more complicated in blends where one component is crystallizable. In such blends the crystalline polymer deforms by having their spherulites change from spherical to ellipsoidal geometry [38–41], resulting in their interlamellar spacing changes. In the situation, the orientation of crystalline lamellae composed of folded chain crystals, arise from the orientation of the folded molecular chains between two lamellae which again show limited relaxation as they are interconnected by the crystal blocks. The amorphous orientation in these blend systems is understood in terms of the conformational changes in the loose molecular chains between crystalline lamellae within a volume-filled spherulitic superstructure [42]. These chains, however, relax to their equilibrium configuration in relatively short times. In addition, the possible temporary networks arising out of the entangled polymer chains inside the interlamellar amorphous region also can contribute to the amorphous orientation upon extension [22,28,42–46].

Poly(butylene terephthalate) (PBT), a commercial engineering thermoplastics, is widely used for its mechanical properties, rapid crystallization rate and excellent moldability. Although PBT is a successful engineering plastic, it has low impact strength and low melt viscosity. In recent years, blends based on the PBT have yielded material of superior properties. One of the most successful commercial polymer blends is that of PBT and polycarbonate (PC). The PBT/PC blends have been commercialized under several trade names such as Xenoy, Makroblend/Pocan and Ultrablend, where PC acts as an effective impact modifier. The published literature confirms that PBT/PC blends are immiscible [47–50]/partial miscible [51–57] at T_g level and are multiphase materials. More important, the investigation showed that PC hinders the PBT-crystallization in PBT/PC blends [58,59]. This, in particular, influences and leads to specific blend morphologies. Consequently these blends are extremely interesting materials in terms of their industrial applications. Such an enormous potential of PBT/PC blends has created the need to characterize the molecular orientation and its relaxation behaviour.

In the present paper we report the segmental orientation and orientation relaxation in uniaxially, stretched films of PBT/PC partial miscible blends. The objective of the present work is to gain further understanding of the orientation behaviour and the molecular mechanisms of deformation in the multiphase polymer blends and to investigate the influence of various aspects of a blend component on the orientation of the other. The PBT/PC blend system also gives the opportunity to study the effect of increasing amount of amorphous content in the blend on the orientation behaviour of the crystallizable component. The information concerning the structural changes in PBT/PC blends induced by the uniaxial mechanical treatment has been derived from the dichroism in the polarization spectra. In the present study, rheo-optical Fourier transform infrared (FTIR) spectroscopy, a technique combining mechanical measurements and linear infrared dichroism spectroscopy has been used for these measurements. This technique allows simultaneous acquisition of stress–strain data and FTIR spectra on-line during mechanical treatment of polymers and successfully applied for the characterization of transient structural changes as a function of time, such as orientation/relaxation, strain induced crystallization and conformational changes, during uniaxial deformation tests or during stress relaxation in very small strain or time intervals [8,60–68]. Both PBT and PC have characteristic absorption bands in their infrared absorption spectrum, which allows one to characterize the individual orientation/relaxation of PBT and PC chains in PBT/PC blends [69–72].

2. Experimental

2.1. Materials

Poly(butylene terephthalate) (PBT) obtained from Aldrich, USA and polycarbonate (PC), a commercial product—Lexan, obtained from GE Plastic, USA were used in this study. PBT has a M_w of 37,000–38,000 and its T_g is 50 °C. PC has a M_w of 40,000 and its T_g is 145 °C.

Pure PBT and PBT/PC blend thin films (of 90/10, 70/30 and 50/50 wt% compositions) were prepared by solution

casting from a 5% ternary mixture of 25% phenol 40% *p*-chlorophenol and 35% 1,1,2,2-tetrachloroethane by weight, on to a optically-flat glass plate. Thin films were prepared by gently heating the blend solution on these glass plates at 95 °C for 30 min. The film samples were then carefully peeled off from the glass plates. Finally, to ensure the removal of residual solvent, blend films were post-dried at 95 °C under vacuum for a week (168 h). It was verified in the infrared spectra that no solvent peaks were present. The sample films, were cut into strips of size 10 mm in length, 5 mm in width. To ensure comparable results all samples stripes measured of pure PBT and PBT/PC blends were taken from the same master-film of about 20 μm in thickness.

2.2. Orientation measurements

The segmental orientation averaged over all chains in a polymer network subjected to uniaxial stretching may be explained by

$$\langle p_2(\mathrm{Cos}\ \theta)\rangle = (3\langle \mathrm{Cos}^2\ \theta\rangle - 1)/2 \tag{1}$$

where θ is the angle between the direction of stretching and the local chain axis of the polymer.

The degree of optical anisotropy in stretched polymer is characterized by the measurement of dichroic ratio, R, which yields the orientation function, f. The orientation function f can be related to the dichroic ratio by expression

$$\langle p_2(\mathrm{Cos}\ \theta)\rangle = f = \frac{(R-1)(R_o+2)}{(R_o-1)(R+2)} = \frac{3\langle \mathrm{Cos}^2\ \theta\rangle - 1}{2} \tag{2}$$

where $R_o = 2\,\mathrm{Cot}^2\ \psi$ is the dichroic ratio for perfect uniaxial order and f corresponds to Herman's orientation function [2,3]. ψ is the angle between the transition vector of the vibrational mode considered and the local chains axis of the polymer. R is the dichroic ratio of the selected absorption band, defined as $R = A_{\|}/A_{\perp}$ ($A_{\|}$and $A_{\perp}$ being the absorbances measured with radiation polarized, respectively, parallel and perpendicular to the stretching direction).

In the cases, where the exact transition moment direction of the considered absorption band is not known, the perfect orientation data can be expressed in terms of the dichroic function DF, proposed by Samules [73].

$$\mathrm{DF} = \frac{R-1}{R+2} \tag{3}$$

Thus, for an absorption band having its transition moment parallel or perpendicular to the chain axis f is given by

$$f_{\|} = \frac{R+1}{R+2} \tag{4}$$

and

$$f_{\perp} = -2\frac{R-1}{R+2} \tag{5}$$

For the parallel chain alignment f becomes 1, for perpendicular alignment 0.5 and for random orientation f becomes 0.

$\langle p_2(\mathrm{Cos}\ \theta)\rangle$, an order parameter is related to the structural absorbance $A_0 = (A_{\|} + 2A_{\perp})/3$ by

$$\langle p_2(\mathrm{Cos}\ \theta)\rangle = F(\Psi) = \frac{A_{\|} - A_{\perp}}{A_{\|} - 2A_{\perp}} \tag{6}$$

where $F(\psi)$ is a probability distribution function for the transition moment direction.

Values of these parameters for the specified absorption bands of the individual spectra were determined by a procedure correlating the successfully calculated absorbance values $A_{\|}$ and $A_{\perp}$. The structural absorbance was chosen as an intensity parameter as it eliminates the influence of changing orientation on the actual intensity of an absorption band [4,60,61].

The spectra series taken on-line to the stretching of PBT, and PBT/PC blends have been evaluated in terms of the structural absorbances (A_0) of the specified characterized internal absorption bands. The transient changes of an amount and anisotropy of the crystalline and amorphous regains in PBT were derived from the structural absorbances of the 1473 cm^{-1} (CH_2 deformation in crystalline region) and 1578 cm^{-1} (symmetric stretching vibration of the phenylene ring in the amorphous region) absorption bands, respectively. The changes in the population of *gauche* (α-form) and *trans* (β-form) conformers of the $-OCH_2CH_2O-$ moiety of PBT chain were monitored by the peak-maximum structural absorbances of 1458 and 956 cm^{-1} infrared absorption bands [69–71]. An aromatic-ring absorption band at 1505 cm^{-1} is insensitive to the changes in the conformational state of order and has been used as internal standard for sample film thickness normalization [74,75]. For PC in blends, the band at 1364 cm^{-1}, assigned to the in phase symmetrical bending vibration of the two methyl groups, has been used to evaluate the orientation of the PC chain segment [72].

2.3. Rheo-optical FTIR spectroscopy

The rheo-optical measurements were carried out employing a variable-temperature and computer controlled electro-mechanical films-stretching device mounted in the sample compartment of a Brucker IFS88FTIR spectrophotometer. The device developed by Siesler has been described in detail elsewhere [62]. The pure PBT, and PBT/PC blend sample films with a gauge dimensions of 10 × 5 mm and a thickness of 20 μm were uniaxially mechanically stretched at constant strain rate ($\varepsilon = 0.01\ \mathrm{s}^{-1}$) and at selected temperatures. Once a desired draw ratio (λ =1, 2 and 3) is achieved, the film samples are allowed to relax in the sample compartment for 360 s. Both the stretching and the following relaxation were made in consecutive steps at same constant temperature and strain rate. A pneumatically rotatable wire-grid polarizers (SPECAC) controlled by the computer, alternating adjust the polarization direction of the

incident radiation parallel and perpendicular to the stretching direction by rapid 90° rotation. The change of the polarization direction in automatically initiated by the last scan of each spectrum. The total number of 10 scans per second is acquired at a resolution of 4 cm^{-1} and a mirror velocity of 10 cm/s. In order to keep uniformity in stretching temperature which allows the correlation of temperature sensitive orientation/relaxation data, the measurements for pure PBT and PBT/PC blends were made at a particular temperature, (T_g(PBT) + 30) °C. This temperature (80 °C) seems to be good reference temperature in present study for a maximum observed elongation ($\lambda = 3$) and for all the investigated PC concentration range in PBT/PC blends. The choice of this temperature, through reasonable higher than the T_g of PBT, leads to faster relaxation and smaller orientation functions of PBT in blends but allows to obtain the uniformity of stretching with pure PBT. Otherwise, with increasing PC concentration in blends, it was difficult to stretch the blend films at lower temperature than this (80 °C), due to sample breakage and uneven stretching. In addition to provide a better and more detailed understanding of orientation/relaxation behaviour of the pure PBT films were also stretched at lower temperature, ($T_g + 5$) °C, 55 °C.

A specially designed software [76] was developed to manage the large number of spectra collected during a rheo-optical experiments. The software treats the collected data in terms of transformation to absorbance spectra, normalization to a suitable reference band, calculation of the dichroic ratio and the orientation function as a function of strain or time. In the present case, the stress/time data points are collected at the rate of ca. 1 data points per second, independently of the infrared spectra and are then converted to the corresponding stress–strain diagram. In the different stress and orientation function profiles, the first part of the curve represents the stress or chain orientation occurring during stretching up to desired elongation. The maximum of stress or orientation at the onset of stress relaxation corresponds to the end of stretching program and thereafter the second part of the curves reflects the chain relaxation at particular elongation.

2.4. Thermal analysis

Differential Scanning Calorimetry (DSC) was carried out on a Perkin Elmer DSC7 operating on UNIX platform under continuous nitrogen flow. DSC was calibrated using an Indium standard (melting temperature $T_m = 156.4$ °C and enthalpy of fusion $\Delta H = 288.40$ J/g). The sample mass was kept constant (5 mg of PBT) throughout the study. The cyclic heating and cooling scans were performed between 40 and 250 °C with a heating/cooling rate of 10 °C/min with retention time of 3 min at 250 °C. The T_g values were defined at the midpoint of the specific heat steps while crystallization and melting temperatures were defined at the maxima of the DSC peaks. The corresponding enthalpy changes, ΔH_f, and ΔH_c were obtained from peak area integration. The weight percentage crystallinity of PBT, in pure PBT and in unstretched and stretched blend films was calculated using 142 J/g as the melting enthalpy for 100% crystallized PBT [77].

Dynamic mechanical thermal analysis (DMTA) were carried out with a direct reading Rheovibron (DDV II-C, model Rheo-200) at 11 Hz as a oscillatory frequency. The changes of storage (E') and loss (tan δ) moduli were measured over the temperature range of 40–180 °C at a heating rate of 3 °C/min. The solution cast films samples of size 5 mm × 15 mm, thickness ca. 30 μm were used for measurements.

3. Results and discussion

3.1. Miscibility of PBT/PC blends

Although the large number of studies have been reported on the miscibility behaviour of PBT/PC blends, many of these have drawn different conclusions [47–57]. It ranges from complete immiscibility when cast from the limited range of available common solvents [47–50] to partial miscibility when melt blended [51–57]. Such a complex behaviour is attributed to liquid–liquid phase separation, crystallization of the PBT and the possible interfacial transesterification reactions.

In the present case the miscibility of the PBT/PC blends is characterized by employing DSC and DMTA techniques. The transitional melting and crystallization behaviours are used to gain insight into the state of miscibility of these blend systems. Fig. 1 shows the DSC heating and cooling thermograms of pure PBT and PC homopolymers and their PBT/PC blends. The presence of two T_g values which are almost identical to those of the two pure components of the blend indicates that the PC may not be completely miscible with semicrystalline PBT. On the other hand, the observed depression of the PBT crystallization temperature (T_c) is attributed to composition dependent growth process of crystallites in the blends [74]. The results obtained from a highly sensitive DMTA technique are shown in Fig. 2. The curves in Fig. 2 show storage modulus (E') and damping (tan δ) verses temperature data for pure PBT, PC and PBT/PC blends. The PBT/PC blends show two relaxation transition peaks located at 155 °C and the other at 55 °C, both in mechanical damping (tan δ) and storage (E') module curves. These peaks (tan δ) corresponds to the T_g values of pure PC and pure PBT, respectively, indicating the presence of an essentially pure PC and PBT phase in blends. A concomitant drop in storage modules (E') curves occurs at similar temperatures. However, a very intriguing feature of these more resolved DMT damping curves for these PBT-rich blend materials is a comparatively broadening of the damping peaks. Apart from this broadening of damping peaks, a low magnitude new relaxation peak is observed in

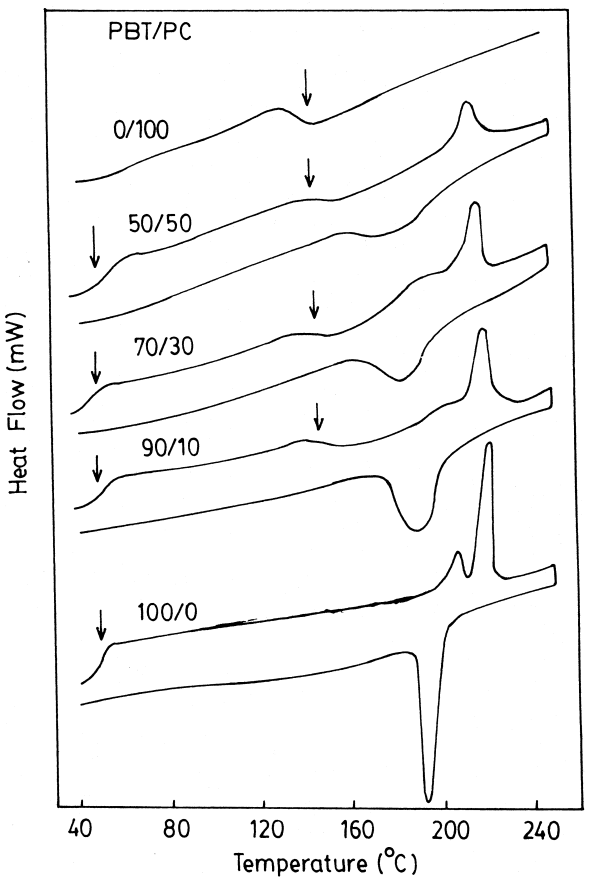

Fig. 1. DSC scans first run curves for PBT, PC and PBT/PC blends. Arrows indicate the position of the glass transition temperatures, T_g's.

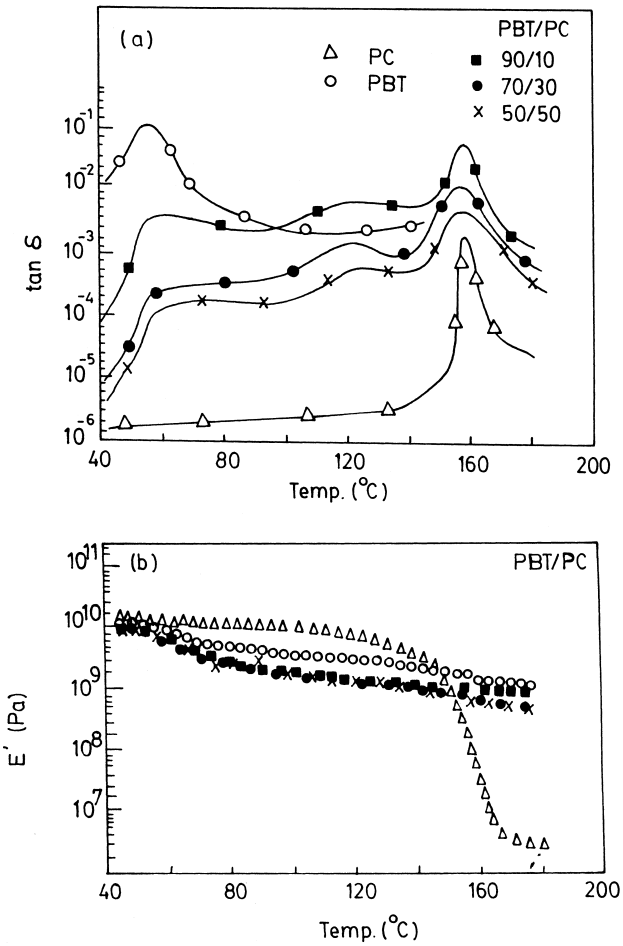

Fig. 2. Dynamic storage modulus (E') and mechanical damping (tan δ) curves for the PBT, PC and PBT/PC blends.

the temperature range of 100–120 °C. Evidently, this peak is an indicative of an amorphous phase, containing both PBT and PC in proportions that critically depend on overall blend compositions and the conditions during the preparation of the blends. On this basis, there would appear to be multiple amorphous phases, with at least one, which contain homogenous blends of the PBT and PC polymers. This view is well supported by the melting and crystallization behaviour of PBT blends

Table 1 gives melting and crystallization characteristics of PBT/PC blends. Both the melting temperature (T_m) and the crystallization temperature (T_c) of PBT crystalline phase are depressed by the presence of PC compared to that of neat PBT. Similarly the heat of fusion (ΔH_f) and heat of crystallization (ΔH_c) of PBT markedly affected at all the three PBT/PC blend compositions, under present investigation.

The observations reported here for PBT/PC blends suggest that the PBT/PC blend samples used in present investigations are certainly not totally immiscible but there is a definite degree of partial miscibility. Thus it is concluded that the present PBT/PC blend samples prepared with described experimental conditions and particularly with present solvent, are essentially multiphase materials, with at least one PBT/PC mixed amorphous phase.

3.2. Crystallinity of PBT in PBT/PC blends

The degree of crystallinity of PBT in the PBT/PC blends is an important parameter, which will considerable affect the stress–strain behaviour and then the orientation–relaxation behaviour during uniaxial deformation. In the present case the crystallinity in solution-cast blend samples, which were used for uniaxial deformation, has been calculated employing DSC technique. The PBT exhibits a large endotherm (Fig. 1) corresponding to a degree of crystallinity of about 31% while the blends with increasing PC content results in the smaller endotherms, indicating a lower degree of crystallinity ranging from 22% in 90/10 PBT/PC blend to 12% in 50/50 composition (Fig. 3). The depression in the PBT crystallinity in unstretched and stretched blends is due to the effects of geometrical constraint of growth provided by the PC domains in PBT/PC immiscible blends [58,59], which affect the formation of various amorphous phase states in the blends. Also, this is in agreement with the observed partial miscible state for the present PBT/PC blends [78]. The degree of PBT crystallinity in blends and so the amount percentage of crystalline and total amorphous

Table 1
Differential Scanning Calorimetry data of PBT/PC Blends

PBT/PC wt.%	T_m (°C)	T_1 (°C)	T_2 (°C)	ΔH_f (J/g)	T_c (°C)	T_3 (°C)	T_4 (°C)	ΔH_c (J/g)
100/0	223.46	215.33	227.60	43.92	194.77	203.60	189.20	48.45
90/10	219.19	205.56	222.46	31.47	187.33	197.86	175.33	41.09
70/30	217.92	201.23	221.50	29.67	185.92	190.50	164.06	32.26
50/50	216.78	204.70	219.86	17.32	184.62	189.53	147.16	15.75

T_m = Melting temperature of the PBT crystalline phase; T_c = Crystallization temperature of the PBT; ΔH_f = heat of fusion of the PBT crystalline phase; ΔH_c = heat of crystallization of the PBT crystalline phase; T_1 = Temperature at the onset of melting; T_2 = Temperature of the completion of melting; T_3 = Temperature at the onset of crystallization; T_4 = Temperature of the completion of crystallization.

materials in the different blend compositions are given in Table 2.

3.3. Orientation and relaxation in stretched pure PBT

The corresponding transient variations in the amorphous and crystalline regions are illustrated in terms of the orientation functions of 1578 and 1473 cm^{-1} absorption bands, respectively (Fig. 4). A significant increase in the orientations of the amorphous and crystalline regions are observed during the stretching procedure at 55 °C. The induced degree of orientation is much larger for the crystalline segments compared to the amorphous segments. This increase in orientation is most pronounced in the strain regain between 20 and 45% strain (Fig. 4), where neck formation move past the sampling area of the infrared beam. It reaches a plateau after 75% strain. Here the PBT reaches the final state of fibrillar orientation in which *c*-axis is aligned parallel to the stretching direction while the *a* and *b*-axes are oriented perpendicular. However, stretching at higher temperature of 80 °C, a significant decrease in the orientation of amorphous regain is observed. Also at this temperature, the orientation of the crystalline regain upon elongation is less than that at 55 °C. This has been understood in terms of relaxation phenomena arising due to increased molecular mobility at higher temperature [79]. Moreover, the reduced structural absorbance of 1578 cm^{-1} (Fig. 5) band suggests that stretching is sensitive to conversion of the amorphous phase to crystalline phase.

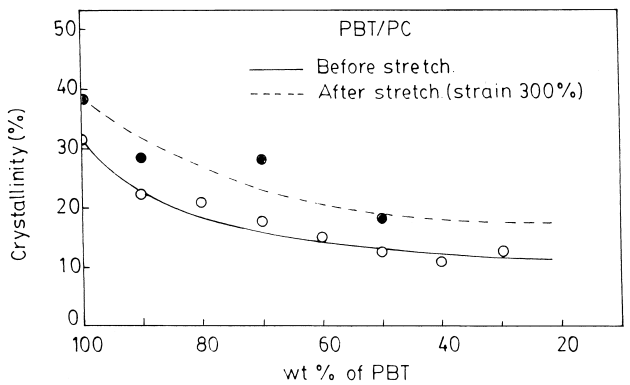

Fig. 3. Crystallinity variation of PBT, before and after film stretching (strain 300%) as a function of PBT content in PBT/PC blends.

Consequently, the 1473 cm^{-1} band exhibits enhancement in structural absorbance with increasing strain. The increased structural absorbance of 1473 cm^{-1} band indicates the strain induced crystallization during stretching in PBT. However, an overall low orientation of remaining amorphous PBT suggests that the interchain entanglements are of complex nature [42]. The rapid decrement in the orientation function of 1578 cm^{-1} absorption band indicates that the amorphous phase also consist of unattached chains [42].

Predominantly, PBT undergoes a stress-induced reversible/non-reversible crystal–crystal phase transition [69,80]. Under tension, the crystal structure of PBT changes from a crumpled near *gauche–trans–gauche* conformation of the aliphatic chain segments (α-form) to an extended

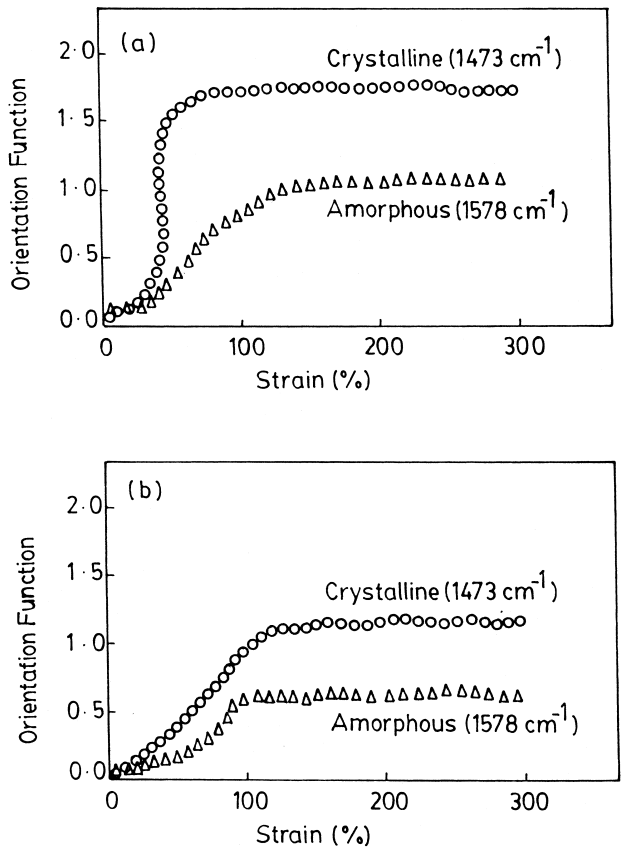

Fig. 4. Orientational changes of the crystalline and amorphous regions of PBT as a function of strain observed during uniaxial deformation at (a) 55 and (b) 80 °C.

Table 2
Differential Scanning Calorimetry data for pure PBT and PBT/PC blends

PBT/PC wt.%	ΔH_m J/g	Crystallinity % in blend		Actua l% of crystalline portion of PBT in blends		Total amorphous % contact in PBT/PC blend	
		Before stretch	After stretch	Before stretch	After stretch	Before stretch	After stretch
100/0	43.92	31	38	31	38	69	62
90/10	31.47	22	28	20	25	80	75
70/30	29.67	21	28	15	25	85	75
50/50	17.32	12	18	06	09	94	91

phase with an all-*trans* sequences (β-form) [56,76]. In fact, this solid-state transformation between the two triclinic crystal structures characteristically affects the mechanical properties of PBT. The absorption bands at 1458 and 956 cm^{-1}, associated with vibrations of aliphatic segment in the relaxed and strained modification, respectively, have been utilized to quantitatively represent the crystal phase transformation as a function of mechanical treatment. In the present case it is observed that upon stretching the structural absorbance of the 1458 cm^{-1} absorption band representing the *gauche* conforms of the crystalline α-modification, drastically decreases whereas the structural absorbance of 956 cm^{-1}-band, corresponding to all-*trans* conformers, exhibit relative increase. The structural absorbance ratio A_0956/A_01458 evaluated from these polarization spectra monitored during the loading–unloading cycle at 55 and 80 °C temperature are plotted as a function of strain in Fig. 6. In both the cases, an increase in the *trans*/*gauche* ratio can be observed in the vicinity of the yield point (Fig. 6). Apart from an initial small reversible position of the phase transition, this conformational transition, in the present case, is of irreversible nature, where the *trans*/*gauche* proportion do not revert to the initial values of the original sample upon unloading (Fig. 6).

Such a deformation behaviour consequently transforms the initial lamellar structure of PBT into a micro fibrillar structure with the fibre axis (*c*-axis) aligned parallel to the stretching direction [81,82]. These fibrils consists of highly aligned PBT-chains which are pulled out from the highly tilted PBT lamellae. During the process of increasing stretching these lamellar domains undergo structural rearrangement eventually resulting in the break up smaller blocks of folded chains, which are then incorporated in the micro-fibrillar structure [42,83,84]. The effect of this morphology is well reflected in the stress–strain curves for elongation recovery cycle during stretching. Fig. 7 shows the stress–strain diagram monitored during stretching of pure PBT at 55 and 80 °C. An initial step rise of stress with strain is followed by a yield point area followed by a flat portion that continues until fracture occurs. It is observed that stretching temperature enhancement above T_g is accompanied by a decrease of stress level with diffused yield point about 40–70% strain. During both the stretching temperatures, however, a neck formation was observed which propagated over about $\lambda = 1$ strain region. Here under the constant force the yield point propagates in the stretching direction. Apart from an initial small stress relaxation, it is observed that the induced strains are permanent deformation as non-recoverable at zero stress (Fig. 4). The non-reversibility of the conformational changes in the present case may be understood in terms of the entanglements of crystalline segments in the amorphous matrix.

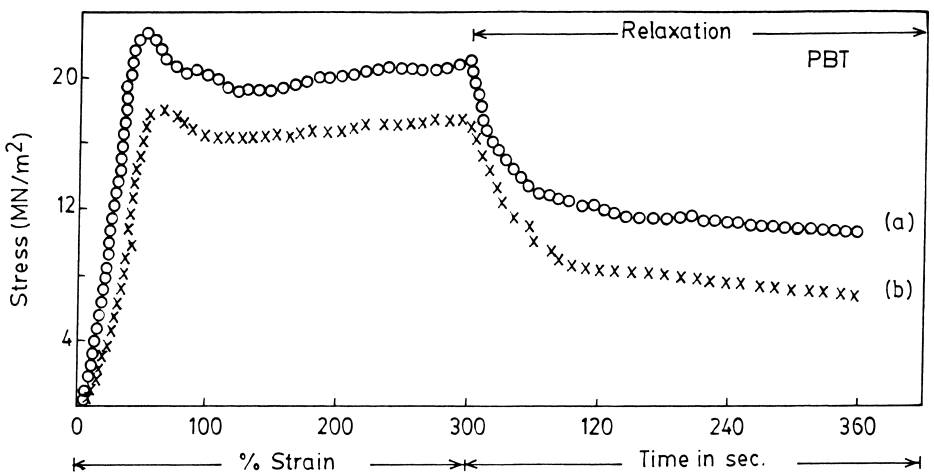

Fig. 5. Stress–strain diagram of the PBT, monitored during successive stress loading–unloading cycle at (a) 55 and (b) 80 °C.

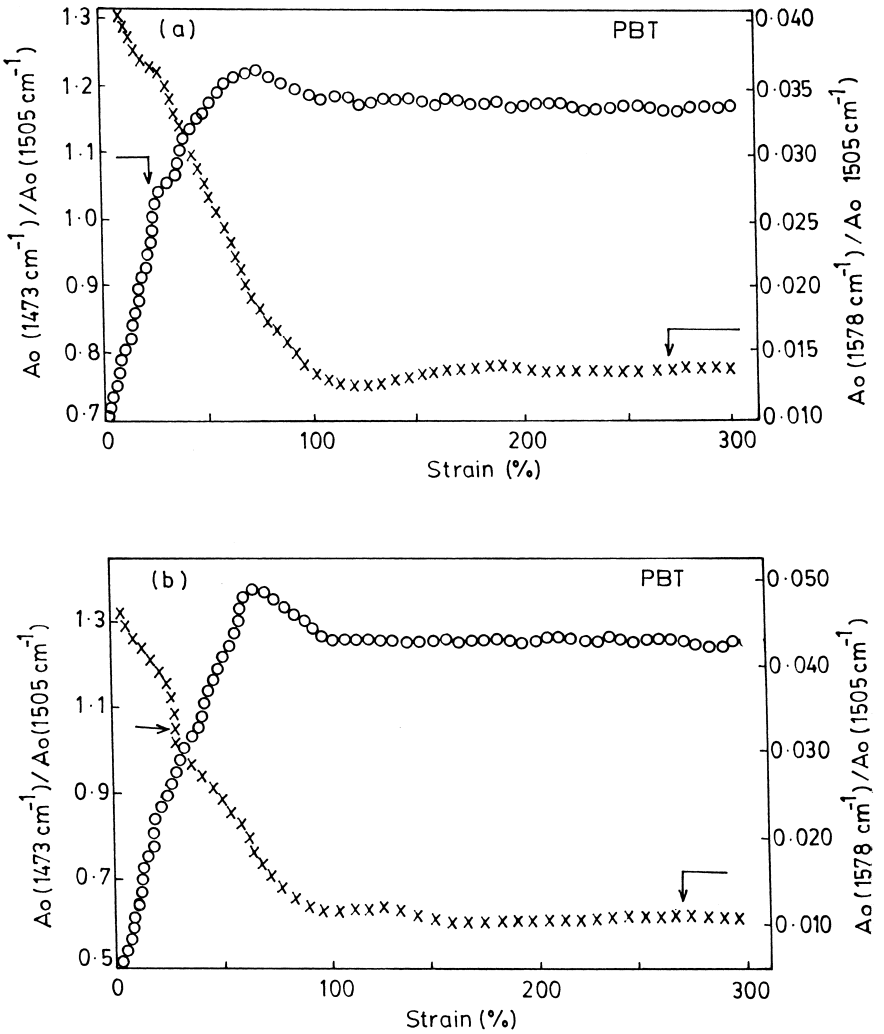

Fig. 6. Plot of the structural absorbance ratios (a) A_0(1473 cm^{-1})/A_0(1505 cm^{-1}) and A_0(1578 cm^{-1})/A_0(1505 cm^{-1}) and (b) A_0(1473 cm^{-1})/A_0(1505 cm^{-1}) and A_0(1578 cm^{-1})/A_0(1505 cm^{-1}), as a function of strain of PBT, derived from the polarization spectra monitored on-line during uniaxial deformation.

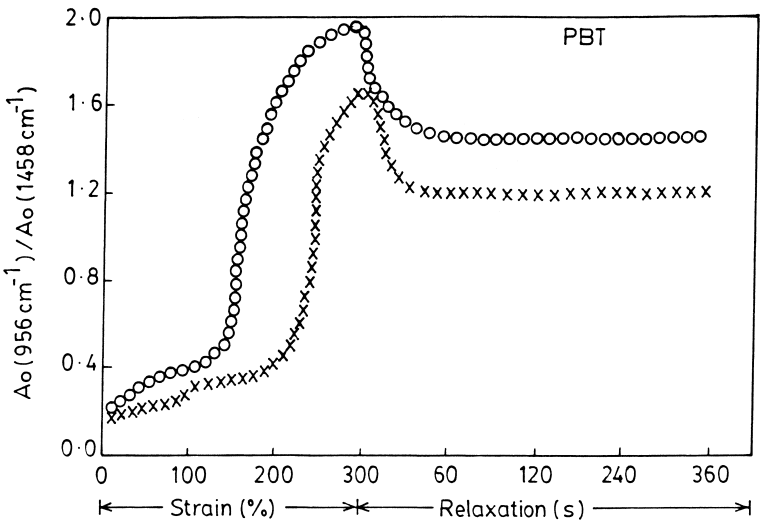

Fig. 7. Changes in the structural absorbance ratios of the *trans*/*gauche* (956 cm^{-1})/A_0(1458 cm^{-1}) absorption bands of PBT as a function of strain, monitored during successive stress loading–unloading cycle, at 80 °C.

3.4. Orientation and relaxation in stretched 90/10 PBT/PC blends

Fig. 8 shows the orientation functions of 90/10 composition of PBT/PC blend stretched at $(T_g + 30)$ °C. It is seen that the segmental orientation of PC chains in blend, represented by 1364 cm^{-1} absorption band, which is totally amorphous in present case, is initially ($\lambda \leq 0.01$) higher than that of amorphous as well as the crystalline orientation of PBT. On the other hand, the segmental orientation of amorphous PBT chains represented by 1578 cm^{-1} absorption band, exhibits higher orientation than the crystalline orientation represented by 1473 cm^{-1} band which is lower in comparison with pure PBT. This behaviour is attributed to the particular morphology of the 90/10 PBT/PC blends. It is known that with low PC concentration in PBT/PC immiscible blends, the amorphous PC is incorporated in the interlamellar spacings of the volume-filling PBT spherulites which ultimately thicken the amorphous layers in interlamellar spacings [54,85,86]. Moreover, the blending of PC with PBT lowers the degree of crystallinity of PBT in blends (Fig. 3). This increases the total amorphous material content in the interlamellar region to 80% of the total weight of the 90/10 PBT/PC blend. The orientation results show that at such small elongations PBT spherulites do not deform but only move in the stretching direction and thus it seems that at this lower strain, the stretching of amorphous chains in blend is a main process which contribute dominantly to the sample elongation. In the case of higher orientation of amorphous PC chains than the amorphous PBT chains, the stretching temperature is an important parameter. In the present case, the stretching is performed at a higher temperature, $(T_g + 30)$ °C compared to T_g of PBT, resulting in greater chain mobility and thus the faster relaxation of the oriented PBT chains than the PC chains in blend.

Further, it is observed that the crystalline orientation function increases rapidly upon extension to $\lambda = 1.00–2.00$ in 90/10 PBT/PC blends, indicating a high segmental orientation of PBT crystalline chains along the stretching direction. However, still the crystalline orientation function of PBT in 90/10 PBT/PC blend is lower than that of the pure PBT (Fig. 8). It seems that compared to pure PBT, the achieved strain is less efficient during the distribution of applied stress between the PBT and PC in transforming the PBT lamellar into microfibrillar structure in the blend. However, at this stage ($\lambda = 2.0$), the result of neck formation in the stretched sample shows that despite the increasing volume of amorphous content in blend the present stretching ($\lambda = 2.0$) remain still effective for deforming the PBT lamellar structure, supporting the most of the extensional force. On the other hand, the segmental orientation of amorphous PBT chains is now much higher compared to PC chains in blend.

Such an orientation behaviour of PBT in 90/10 PBT/PC blend may be understood in terms of PBT-spherulites deformation upon stretching. Starting the uniaxial stretching, the spherulites initially deform and then lamellae placed within the spherulite cavities, composed of loose chain folds, tie chains cilia and other unattached chains, are transformed into microfibrils. The process ultimately results in a neck formation. The cilia, loops or unattached chains are expected to orient less than the crystal block interconnected tie chains as they relax back toward their equilibrium configuration in relatively short times [42]. In the present case the results in figure suggests that the amorphous regions represented by *gauche* conformers (1578 cm^{-1}) in the PBT includes in majority number of cilia, loops or unattached chains which contribute to the elongation-induced amorphous orientation. Sometimes, the microcrystalline PBT segments in 90/10 PBT/PC blend, represented by *trans*-conformers (1473 cm^{-1}) in PBT, interconnected by the tie chains tends to maintain their

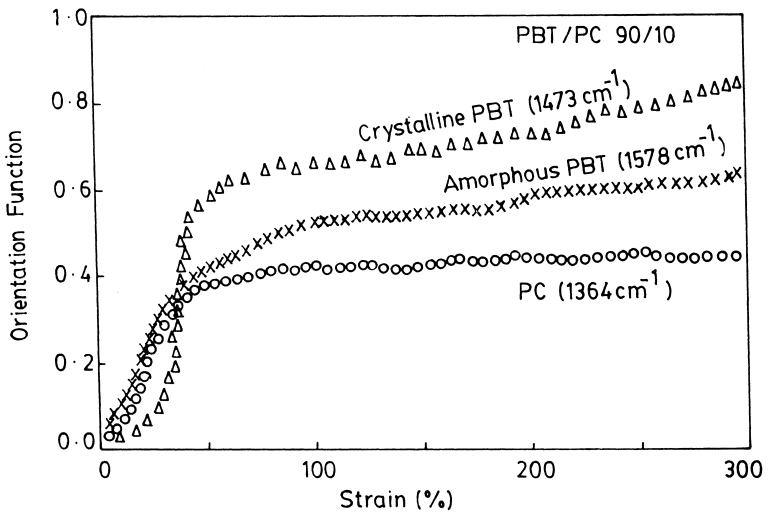

Fig. 8. Orientational changes of the crystalline and amorphous regions of PBT and amorphous PC in 90/10 PBT/PC blend, as a function of strain, observed during uniaxial deformation, at 80 °C.

segmental orientation. The overall lower orientation of PC chains in blend is proposed to be attributed to the stretching temperature. When the stretching temperature is above the T_g of the major phase, the applied stress only deforms the minor phase into sub-domains [29]. This leads to a lower or no orientation. Therefore it is expected that the PC chains in 90/10 PBT/PC immiscible blend stretched at lower temperature than the T_g of PC (145 °C) exhibits a low orientation.

Further the 90/10 PBT/PC blend is stretched to $\lambda = 3$ (Fig. 8). The very high PBT crystalline orientation observed for the blend indicates that now the structural transformation of the crystalline PBT from lamellae to microfibrils dominates the stretching process. The structural absorbance of the absorption band, 1458 cm^{-1}, belonging to the crumpled α-form of PBT drastically decreases whereas the 956 cm^{-1} band, representing the extended phase with all-*trans* absorbance sequence, exhibits relative increase in absorbance. Similar to pure PBT an increase in the *trans*/*gauche* ratio can be observed in the vicinity of the yield point (Fig. 9). This implies to the formation of a fibrillar structure with all *trans*-conformation of the aliphatic segments (Fig. 9). As similar to the stress–strain relaxation behaviour of 90/10 PBT/PC blend (Fig. 9), the conformational transition is irreversible where the intensity of the absorption band 1458 cm^{-1}, do not completely revert back to its initial value. Comparing the increase in intensity of absorption band 1458 cm^{-1} in 90/10 PBT/PC blend with that of pure PBT during relaxation of stress is of interest. In the case of the blend the intensity of this band and thus the induced strains are much higher recoverable than in pure PBT. This suggests a distinct influence of the increased amorphous content upon PC blending on the relaxation behaviour of PBT. It is reasonable to expect that, now the tie chains which interconnect the PBT crystal blocks in PBT/PC blend could store lower residual stress compare to pure PBT due to enhanced chain mobility, resulting in faster relaxation of *trans–gauche–trans* conformational transition. Nevertheless, still this lower non-reversibility of the phase transition in blend is efficient, to transform the lamellae into microfibrillar structure during uniaxial stretching.

3.5. Orientation and relaxation in stretched 70/30 and 50/50 PBT/PC blends

The rheo-optical experiments were performed by stretching 70/30 and 50/50 PBT/PC blend films. These films were directly stretched to $\lambda = 3$ at $(T_g + 30)$ °C. The results show in Fig. 11 for 70/30 blend composition suggest that the orientation function behaviour of the amorphous PBT and the PC chains is similar to that observed for 90/10 blend composition. The achievable orientation functions of these two amorphous components are of lower values compared to that found for 90/10 blend. As mentioned earlier the incorporation of PC hinders the crystallization of PBT in blends. The 70/30 blend films shows a PBT crystallinity degree of 21% resulting in 15% the total weight of crystalline and 85% total amorphous material in blend. In such a case possible initiation of the chain entanglements between the PBT and PC amorphous region may contribute to the lower orientation/relaxation, supporting most of the stress upon extension. However, the tie chains of amorphous PBT in the interlamellar region which are interconnected by the crystal blocks also contribute to this overall limited orientation relaxation.

It is interesting to observe that, in spite of decreasing the degree of crystallinity of PBT in blend, in stress–strain diagram (Fig. 10), the blend still show a prominent yield point at about 50–55% strain with decreasing stress level and to some extent diffused in nature. The blend film, however, still exhibits neck formation upon stretching. The observed PBT crystalline orientation is little lower compared to that of the PBT in 90/10 PBT/PC blend (Fig. 11).

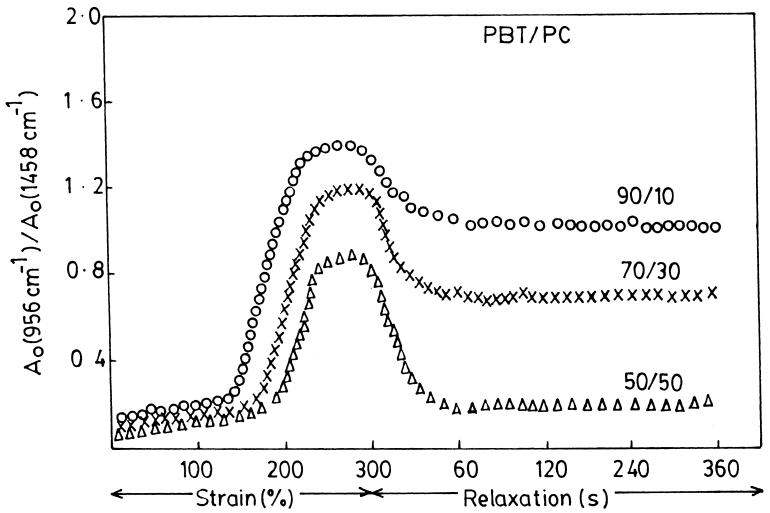

Fig. 9. Changes in the structural absorbance ratios of the *trans*/*gauche* $((956\,cm^{-1})/A_0(1458\,cm^{-1})$ absorption bands of the PBT in 90/10, 70/30 and 50/50 PBT/PC blends, as a function of strain monitored during successive stress loading–unloading cycle at 80 °C.

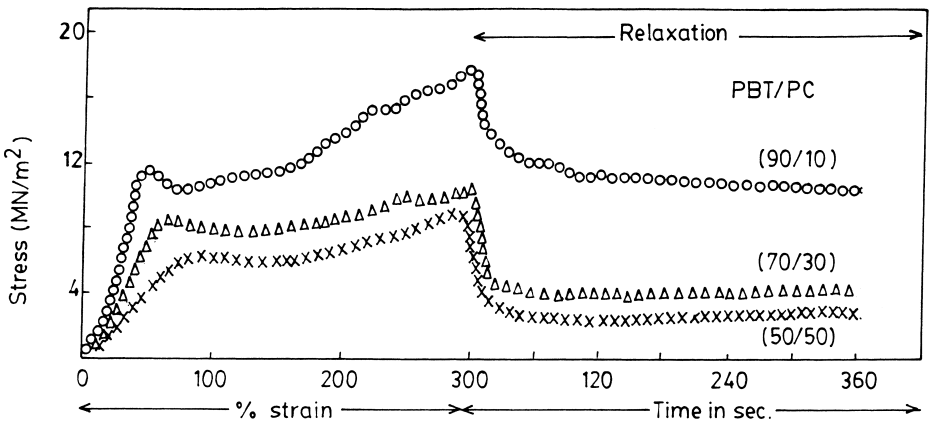

Fig. 10. Stress–strain diagram of the 90/10, 70/30 and 50/50 PBT/PC blends monitored during successive stress loading–unloading cycle, at 80 °C.

This may be attributed to the influence of the increasing volume (85%) of the amorphous regain in the blend. The morphology of the 70/30 blend, however, show usual PBT spherulitic structure [85].

Further in 70/30 blend, PC is in its amorphous state and exists in the interlamellar regain of less-volume-filling PBT spherulites [85]. With such a blend morphology where the dominant amorphous proportions are expected to support most of the stress, it seems that still the stretching remains effective and transforms the PBT lamellar to microfibrils in the blend, through PBT crystal block-interconnected oriented tie chains. However, in rheo-optical spectra (Fig. 9) the absorption band 1458 cm^{-1}, compared to 90/10 blend, exhibits higher structural absorbance. This implies to low conversion of α-form to *trans*-β-form in the blend, indicating less-efficient transformation of the lamellar to the fibrillar structure. Upon recovery to zero stress the increased reversibility of this phase transition may be understood in terms of the decreased entanglement of PBT crystalline segments in the larger amorphous matrix in the 70/30 blend.

In 50/50 PBT/PC blend, the crystalline PBT account for 6% the total weight of the blend. The remaining 94% is together amorphous PBT and PC. Significant change in the morphology of PBT/PC blend has been reported with the increasing weight percentage of PC. In 50/50 blend, the crystalline structure of PBT is observed to consist of non-spherulitic, sheaf like packet of lamellar, which even penetrates into the PC domains. The PC trapped within the crystalline PBT phase inhabits PBT spherulite formation [59,85]. With increasing PC concentration in the blend the dispersed PC phase forms an interpenetrating network. Such a morphology has a significant effect on the deformation behaviour of 50/50 PBT/PB blend.

The stress–stain diagram of 50/50 PBT/PC blend is shown along with 90/10 and 30/70 blend compositions in Fig. 10. Apart from the substantial reduction of the stress level due to increased PC content in the blend which is again a indicative of the miscibility or at least partial miscibility in present PBT/PC blend samples, the most obvious feature is the very diffuse nature of the yield point at about 70% strain. However, the neck formation was observed which propagated over the total sample area and completed before

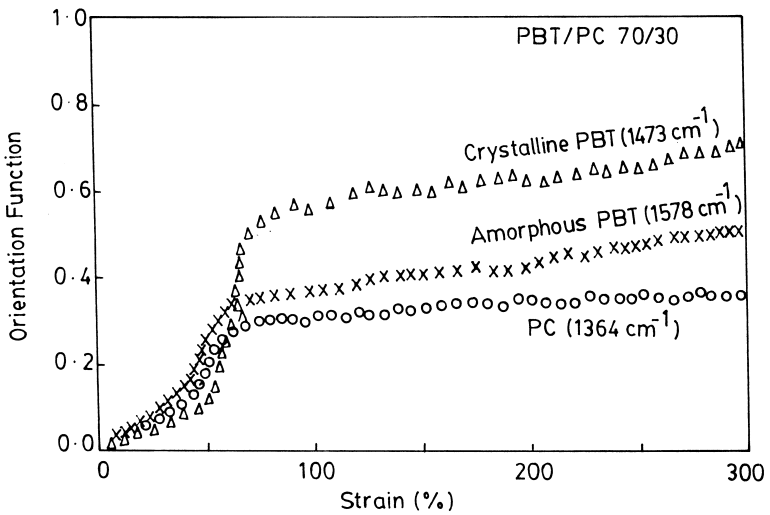

Fig. 11. Orientational changes of the crystalline and amorphous regions of PBT and amorphous PC in 70/30 PBT/PC blend, as a function of strain, observed during uniaxial deformation, at 80 °C.

completing the stretching, $\lambda = 3$. Fig. 12 shows the orientation functions of crystalline (1473 cm^{-1}) and amorphous (1578 cm^{-1}) PBT and PC (1364 cm^{-1}) in 50/50 blend. Even with few PBT crystal domains present before stretching in the blend, substantial crystalline orientation of PBT is observed (Fig. 12). As pointed out earlier, upon stretching these crystalline domains breaks off into smaller blocks of folded chains, ultimately resulting in the formation of microfibril like crystallites of PBT, and thus, increases PBT-crystallinity value in stretched PBT/PC film. This is well confirmed by a DSC measurement, which shows a PBT crystallinity degree of 12% before stretching and 18% after stretching in 50/50 PBT/PC blend, (Table 2). The spectroscopic changes corresponding to this structural transformation is observed for the changes in the structural absorbance of 1458 cm^{-1} (α-form) and 956 cm^{-1} (β-form) absorption bands. Upon recovery to zero stress these changes in the structural absorbances are non-reversible (Fig. 9).

Apart from the formation of microfibril-like crystallites of PBT from the exiting lamellae, this observed high crystallization orientation in 50/50 PBT/PC blend is also related to stress-induced-transformation of PBT chains in amorphous PBT-component to *all-trans* extended crystalline form. These PBT-chains have the high potential to form microfibril-like crystallites of PBT [86]. For the representation of spectroscopic effects, the conformational sensitive 1400–1500 cm^{-1} δ $(CH)_2$ regain has been monitored. It is observed that during stretching the structural absorbance of the 1459 cm^{-1} band, corresponding to relaxed α-form in amorphous regain, caused by interaction of the methylene groups adjacent to the oxygen atoms with their neighbourhood, drastically decreases, whereas the structural absorbance of the 1473 cm^{-1} band, assigned to vibrations of the central methylene group in almost planar all-*trans* conformation in extended crystal form, exhibits a relative increase (Fig. 13). These spectral results can be attributed to the structural transformation in the PBT-amorphous regain and ultimately resulting in to the formation of the fibrillar structure of the PBT aliphatic segments. The predominant non-reversible nature of this conformational transition clearly reflects that only small portion of polymer chains reversibly recovering to the crumpled α-conformational upon unloading the stress [87]. This non-reversibility of the conformational changes for the crystalline regains distributed in the amorphous regains may be explained by entanglement of the polymer chains in the amorphous matrix during the elongation process. Thus the formation of microfibrils during the stretching in this 50/50 composition may be attributed to cumulative contribution from the deformation of existing PBT lamellae dispersed in the amorphous PBT/PC matrix and the stress transformation of PBT chains, out of the PBT amorphous regain to all *trans*-conformation in extended crystal form, aligned along the stretching direction.

The orientation of the amorphous PBT is almost similar to that observed for 70/30 blend composition. On the other hand, the orientation of the amorphous PC decreases a little (Fig. 12). These results suggest a distinct effect of the 50/50 blend morphology. The blend forms an entanglement of two interpenetrating network in the interlamellar amorphous regions. Upon stretching such a blend film, it is expected that the stronger and more rigid PBT network will support the stress and will show significant orientation, in the stretching direction. It is more possible that the relaxation of the PBT amorphous chains, which also includes the tie chains, may be hindered by the orientation lamellae of PBT. However, the still relatively observed low orientation value of the amorphous PBT chains than expected indicates that even when blend forms entanglements in the amorphous regain, the stretching the blend shows the interplay between the orientation of the PBT amorphous component and

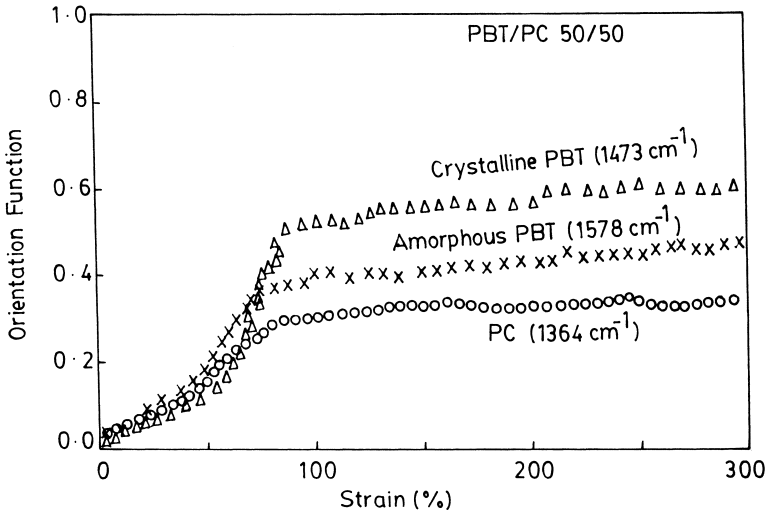

Fig. 12. Orientational changes of the crystalline and amorphous regions of PBT and amorphous PC in 50/50 PBT/PC blend, as a function of strain, observed during uniaxial deformation, at 80 °C.

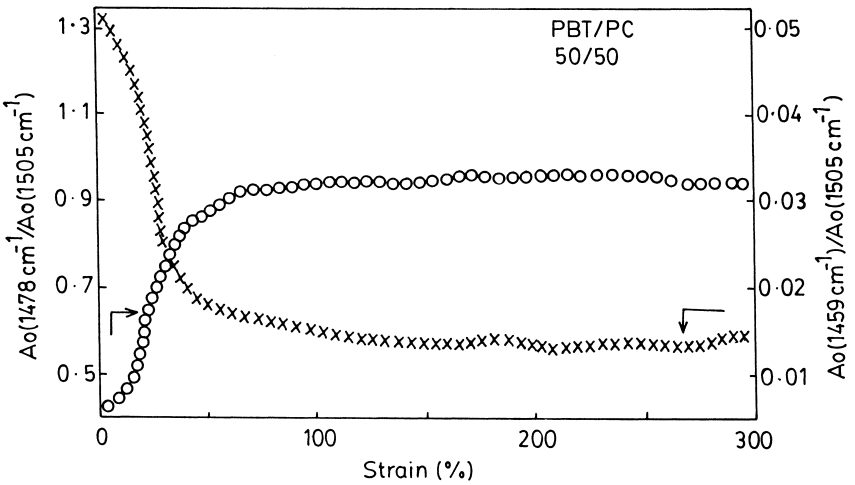

Fig. 13. Changes in the structural absorbance ratios of the absorption bands of relaxed α-form, $A_0(1459\ cm^{-1})/A_0(1505\ cm^{-1})$ in the amorphous regain, and the all-*trans* extended crystalline form $A_0(1473\ cm^{-1})/A_0(1505\ cm^{-1})$ in the amorphous region of PBT in 50/50 PBT/PC blend as a function of strain monitored during uniaxial deformation, at 80 °C.

stress-induced transformation of PBT amorphous chains to all trans crystalline form.

4. Conclusion

Rheo-optical FTIR spectroscopy has been successfully utilized in order to analyse the orientation and orientation relaxation in PBT/PC blends.

For semicrystalline PBT/PC partial miscible blends, the molecular orientation and the deformation mechanism are interrelated to resulting PBT spherulitic morphology and the temporary network formed by the elongated PBT and PC chains inside the interlamellar regions. Compared to pure PBT, the PBT in PBT/PC blend exhibits lower degree of crystalline orientation, and is further lowered by the addition of PC.

In the blends, containing 10 and 30 wt% of PC, for which the spherulites are volume-filling and having a high PBT crystallinity, uniaxial stretching results in the crystalline transformation from lamellae to microfibrils. The predominant formation of this fibrillar structure is due to non-reversibility of an extended phase with all-*trans* conformation of the aliphatic PBT segments occurring during elongation. However, the rate of relaxation of this conformational transition increases with increasing amorphous content in the blends. This limiting relaxation may be due to entanglement of PBT crystalline segments in the amorphous matrix, largely trapped by the orientated interpenetrating tie chains between PBT lamellae.

In the present study, the PBT/PC 50/50 blend, even with as little as 5% amount of crystalline PBT, shows significant perfect segmental orientation for the crystalline PBT, which ultimately leads to the transformation of the few existing lamellae to microfibrils upon uniaxial stretching. In fact, in the present case PBT/PC as compared to unstretched blend films, stretched films show higher degree of PBT crystallinity. This strain-induced transformation of PBT-amorphous chains to all trans extended crystalline form also contributes to an overall PBT-crystalline orientation in blends. This also contributes in further lowering the overall PBT-amorphous orientation, than expected. The results clearly indicates that structural transformation in PBT, still remain the dominant process during stretching of the PBT/PC blends.

For all the PBT/PC blend compositions investigated, the orientation of the amorphous PBT in blends is lower than that of the pure amorphous PBT. The network arising from entangled polymer chains have a distinct influence on the orientation behaviour in the amorphous regions. The restricted relaxation of amorphous PBT and PC chains particularly in the PBT-rich blends is attributed to the trapping of amorphous chains in oriented PBT lamellae.

Acknowledgements

The authors gratefully acknowledge instrumental and financial support of the Deutsche Forschungs gemeinschaft, Germany, and of the Fonds der Chemischen Industrie, Germany, to Professor H.W. Siesler at Department of Physical Chemistry University of Essen, Essen Germany. Dr A.K. Kalkar is grateful to Professor H.W. Siesler for financial support during his visit to University of Essen, Essen Germany.

References

[1] Fakirov S, editor. Oriented polymer materials. Heidelberg: Huthig and Wepf Verlag Zug; 1996.

[2] Ward IM, editor. Development in oriented polymers, vols. 1 and 2. New York: Applied Sciences Publishers; 1982, 1987.
[3] Ward IM, editor. Structure and properties of oriented polymers. London: Chapman and Hall; 1997.
[4] Siesler HW, Holland-Moritz K. Infrared and Raman spectroscopy of polymers. New York: Marcel Dekker; 1980.
[5] Monnerie L. In: Pethrick RA, Richards RW, editors. Static and dynamic properties of the polymeric solid state. Dordrecht: Reidel; 1982. p. 383.
[6] Bokobza L, Amram B, Monnerie L. In: Mark JE, Erman B, editors. Electromeric polymer network. Englewood Cliffs, NJ: Prentice Hall; 1992. p. 289.
[7] Jasse B, Tassin JF, Monnerie L. Prog Colloid Polym Sci 1993;92:8.
[8] Kalkar AK, Siesler HW, Zebger I, Pfeifer F, Ameri A, Michel S, Hoffmann U. Rheo-optical Fourier-transform infrared spectroscopy of polymers. In: Chalmers J, Griffiths PR, editors. Handbook of vibrational spectroscopy. London: Wiley; 2002. p. 2559.
[9] Sott P, Deloche B, Herz J. Makromol Chem Macromol Symp 1991; 45:177.
[10] Sott P, Deloche B. Macromolecules 1990;23:1999.
[11] Lefebvre D, Jasse B, Monnerie L. Polymer 1982;23:706.
[12] Buffeteau T, Desbat B, Besbes S, Nafati M, Bokobza L. Polymer 1994;35:2538.
[13] Archer LA, Fuller GG. Macromolecules 1994;27:4359.
[14] Lafrance CP, Prudhomme RE. Polymer 1994;35:3927.
[15] Kaito A, Kyotani M, Nakayama KJ. J Polym Sci, Polym Phys Ed 1993;31:1099.
[16] Gustafsson G, Inganas O, Osterholm H, Laakso J. Polymer 1991;32: 1574.
[17] de Gennes PG. J Chem Phys 1971;55:572.
[18] Doi M, Edwards SF. J Chem Soc, Faraday Trans 1978;74:1789. See also pages 1802 and 1818.
[19] Doi M, Edwards SF. J Chem Soc, Faraday Trans 1979;75:32.
[20] Bouton C, Arrondel V, Rey V, Sergot P, Manguin JL, Jasse B, Monnerie L. Polymer 1989;30:1414.
[21] Zhao Y, Jasse B, Monnerie L. Polymer 1991;32:209.
[22] Zhao Y, Bazuin CG, Prudhomme RE. Macromolecules 1991;24:1261.
[23] Zhao Y, Jasse B, Monnerie L. Polymer 1989;30:1643.
[24] Chabot P, Prudhomme RE, Pezolet M. J Polym Sci, Polym Phys Ed 1990;28:1283.
[25] Oultache AK, Zhao Y, Jasse B, Monneriel L. Polymer 1994;35:681.
[26] Abtal E, Prudhomme RE. Macromolecules 1994;27:5780.
[27] Kawabata K, Fukuda T, Tsujii Y, Miyamoto. Macromolecules 1993; 26:3980.
[28] Li W, Prudhomme RE. Polymer 1994;35:3260.
[29] Hong SD, Shen M, Russell T, Stein RS. In: Klempner D, Frisch KC, editors. Polymer alloys blends, grafts and interpenetrating networks. New York: Plenum; 1977. p. 77.
[30] Hubbell DS, Copper SL. J Polym Sci, Polym Ed 1977;15:1143.
[31] Lu FJ, Burchell DJ, Li X, Hsu SL. Polym Engng Sci 1983;23:861.
[32] Hsu SL, Lu FJ, Benedetti E. Adv Chem Ser 1984;206:101.
[33] Endo S, Min K, White JL, Kyu T. Polym Engng Sci 1986;26:45.
[34] Kim JH, Karasz FE, Malone MF. Polym Engng Sci 1991;31:13.
[35] Abtal E, Prudhomme RE. Polym Engng Sci 1992;32:1857.
[36] Li W, Prudhomme RE. Polymer 1994;35:3260.
[37] Li D, Brisson J. Macromolecules 1997;30:8425.
[38] Sasaguri K, Hoshino S, Stein RS. J Appl Phys 1964;35:47.
[39] Sasaguri K, Yamada R, Stein RS. J Appl Phys 1964;35:3188.
[40] Hay II, Keller A. J Mater Sci 1966;1:41.
[41] Hay II, Keller A. Kolloid Z 1965;204:43.
[42] Petraccone V, Sanchez IC, Stein RS. J Appl Polym Sci Polym Ed 1975;13:1991.
[43] Zhao Y, Bazuin CG, Prudhomme RE. Macromolecules 1989;22:3788.
[44] Erman B, Monnerie L. Macromolecules 1985;18:1985.
[45] Queslel JP, Erman B, Monnerie L. Macromolecules 1985;18:1991.
[46] Keroack D, Zhao Y, Prudhomme RE. Polymer 1998;40:243.
[47] Hanrahan BD, Angeli SR, Runt J. Polym Bull 1985;14:399.
[48] Wings N, Trafara G. Angew Makromol Chem 1994;217:91.
[49] Kim WN, Burns CM. Makromol Chem 1989;190:661.
[50] Hobbs SY, Groshans VL, Dekkers MEJ, Shultz AR. Polym Bull 1983; 17:335.
[51] Wahrmund DC, Paul DR, Barlow JW. J Appl Polym Sci 1978;22: 2155.
[52] Paul DR, Barlow JW, Cruz CA, Mohn RN, Nassar TR, Wahrmund DC. Chem Soc Org Coat Plast Div Prepr 1977;37:130.
[53] Sanchez P, Remiro PM, Nazabal J. J Appl Polym Sci 1993;50:995.
[54] Delimay D, Goffaux B, Devaux J, Legras R. Polymer 1995;36:3255.
[55] Okamoto, Inaue T. Polymer 1994;35:257.
[56] Wilkinson AN, Tattaum SB, Ryan AJ. Polymer 1997;38:1923.
[57] Dekkers MEJ, Hobbs SY, Bruker I, Watkins VH. Polym Engng Sci 1990;30:1628.
[58] Runt J, Miley DM, Zhang X, Gallagher KP, McFeaters K, Fishburn J. Macromolecules 1992;25:1929.
[59] Tattum SB, Cole D, Wilkinson AN. J Macromol Sci Phys 2000;B39: 459.
[60] Siesler HW. Adv Polym Sci 1984;65:1.
[61] Siesler HW. In: Mackenzie MW, editor. Advances in applied FTIR spectroscopy. Chichester, England: Wiley; 1988. p. 189.
[62] Siesler HW. Makromol Chem Macromol Symp 1992;53:89.
[63] Siesler HW. In: Urban MW, Craver CD, editors. Structure–property relation in polymers: spectroscopy and performances. Advances in chemistry, series no. 236, Washington DC: Am. Chem. Soc. Books Department; 1993. p. 31.
[64] Hoffmann U, Pfeifer F, Okretic S, Volkl N, Zahedi M, Siesler HW. Appl Spectrosc 1993;41:1531.
[65] Kalkar AK, Pfeifer F, Siesler HW. Macromol Chem Phys 1998;199: 667.
[66] Ameri A, Sieler HW. J Appl Polym Sci 1998;70:1349.
[67] Siesler HW. Macromol Chem Symp 1986;5:151.
[68] Gupta VB, Ramesh C, Siesler HW. J Polym Sci Polym Phys Ed 1985; 23:405.
[69] Ward IM, Wilding MA. Polymer 1977;18:327.
[70] Gillette PC, Dirlikov SD, Koenig JL, Lando JB. Polymer 1982;23: 1759.
[71] Siesler HW. J Appl Polym Sci 1979;17:453.
[72] Lunn AC, Yannas IV. J Polym Sci, Polym Phys Ed 1972;10:2189.
[73] Samuels RJ. Makromol Chem Suppl 1981;4:241.
[74] Krimm S. Adv Polym Sci 1960;2:51.
[75] Rao MVS, Dweltz NE. J Appl Polym Sci 1986;31:1239.
[76] Hoffmann U. Unpublished results.
[77] Illers KH. Colloid Polym Sci 1980;258:117.
[78] Pompe G, Meyer E, Komber H, Hamann H. Thermochim Acta 1991; 187:185.
[79] Fajolle R, Tassin JF, Sergot P, Pambrun C, Monnerie L. Polymer 1983;24:379.
[80] Siesler HW. J Polym Sci Polym Lett Ed 1979;17:453.
[81] Siesler HW. Rheo-optical Fourier-transform infrared spectroscopy: vibrational spectra and mechanical properties of polymer. Advances in polymer science, vol. 65. Berlin: Springer; 1984. p. 1.
[82] Glenz W, Peterlin A. J Polym Sci, Part A2 1971;9:1191.
[83] Glenz W, Peterlin A. J Macromol Sci Phys 1970;5:473.
[84] Peterlin A. J Polym Sci, Part C 1965;(9):1965.
[85] Halder RS, Joshi M, Misra A. J Appl Polym Sci 1990;39:1251.
[86] Hobbs SY, Dekkers MEJ, Watkins VH. J Mater Sci 1988;23:1291. See also page 1225.
[87] Holland-Moritz K, Siesler HW. Polym Bull 1981;4:165.